

[Constraining the age and provenance
of the basal quartzites of the
Centralian Superbasin—revisiting the
Heavitree Formation]

Thesis submitted in accordance with the requirements of the University of
Adelaide for an Honours Degree in Geology/Geophysics

[Mohammed Al-Kiyumi]

October 2018

Word count: 5560



THE UNIVERSITY
of ADELAIDE

CONSTRAINING THE AGE AND PROVENANCE OF THE BASAL QUARTZITES OF THE CENTRALIAN SUPERBASIN

The age and provenance of the Heavitree Formation

ABSTRACT

The Heavitree Formation of the Amadeus Basin, central Australia, is thought to correlate with a number of similar formations in the Officer, Ngalia, Georgina and Murraba Basins that formed the Centralian Superbasin. The Jasper Gorge Formation of the Victoria Basin and Jamison sandstone of the Beetaloo Sub-basin are also thought to be corollaries. These formations are all constrained to being younger than ca. 1.0 Ga by U-Pb detrital zircon studies. However, in all cases, this is suspected to considerably pre-date the timing of deposition. Here, we present new U-Pb and Hf data from seven samples of the Amadeus Basin Heavitree Formation to a) better constrain the age of the Heavitree Formation, b) investigate the spatial variation in provenance of the Heavitree Formation, and, c) compare with other ‘Supersequence 1’ quartzites from the wider Centralian Superbasin.

KEYWORDS

Heavitree Formation, Amadeus Basin, Centralian Superbasin, Neoproterozoic quartzites, U-Pb detrital zircon geochronology, Lu-Hf isotopes data.

TABLE OF CONTENTS

Constraining the age and provenance of the basal quartzites of the Centralian Superbasin	i
The age and provenance of the Heavitree Formation.....	i
Abstract.....	i
Keywords.....	i
List of Figures and Tables	3
Introduction	4
Geological Setting	6
The Amadeus Basin and Centralian Superbasin.....	6
The Heavitree Formation.....	7
Methods	9
U-Pb zircon geochronology.....	9
Lu-Hf isotopes determination.....	11
Results	11
U-Pb isotopic data	11
HQ-01	12
HQ-03	13
HQ-04.....	14
HQ-05.....	14
HQ-06.....	15
HQ-08.....	15
BL-002.....	16
Lu-Hf isotopic data.....	18
HQ-01	18
HQ-04.....	18
HQ-05.....	19
HQ-06.....	19
HQ-08.....	19
BL-002.....	20
Rare-Earth-Element analysis in zircon.....	21
HQ-01	21
HQ-03	21
HQ-04.....	21
HQ-05.....	22

HQ-06.....	22
HQ-08.....	22
BL-002.....	23
Discussion.....	23
Maximum Deposition constraints.....	23
Spatial and temporal variance.....	24
Heavitree Formation equivalent formations.....	26
Provenance Analysis.....	27
Conclusions.....	32
Acknowledgments.....	33
References.....	33
Appendix A:.....	36

LIST OF FIGURES AND TABLES

Figure 1: Collected samples locations in the north of the Amadeus Basin. Two Heavitree Formation locations added after Normington et al. (2016) and Kositcin (2014). Modified after Edgoose (2012).	12
Figure 2: Wetherill Concordia plots of all samples analysed.	17
Figure 3: $\epsilon\text{Hf}(t)$ value of samples analysed.	20
Figure 4: Samples comparison in KDE. Additional Heavitree Formation obtained after Normington et al. (2016) and Kositcin et al (2014).	26
Figure 5: KDE plot off all samples collected, Heavitree Formation equivalent sandstones and potential source regions.	30
Figure 6: MDS of all samples collected, Heavitree Formation equivalents and potential source regions.	31

INTRODUCTION

In the Neoproterozoic and early Palaeozoic, large sedimentary basins covered extensive areas southern, central and northern Australia. The Neoproterozoic successions of the Amadeus Basin alongside with the Georgina, Officer former Savory and Ngalia basins comprised a single, widespread intracratonic depositional system named the Centralian Superbasin, contiguous with the Adelaide Fold Belt in South Australia. Other basins such as Victoria and Murraba basins have been added afterwards (Munson et al. 2012). The Heavitree formation and the Dean Quartzite together with the overlying Bitter Springs Formation form the 'Supersequence 1' of the Centralian Superbasin (Edgoose 2012). Quartzites in other basins are argued to be correlated to the Heavitree Formation, which supports the concept of the Centralian Superbasin. However, the correlation is done merely by the stratigraphic position of these units as they all rest unconformably above a basement and are overlain by a thick evaporite sequence (Plummer 2015).

The Tonian Period (1000–860 Ma) of the Neoproterozoic Era is recorded in several quartzite units in Australia. One of those is the basal unit of the Amadeus Basin the Heavitree Formation. It is an extensive, sheet-like and uniform deposit that was deposited in in high energy shelf-like environment (Edgoose 2012). The Heavitree Formation, and its equivalent the Dean Quartzite, are largely exposed in the northern and southwestern margins of the present-day Amadeus Basin. Both, the intrusion of Stuart Pass dolerite into the Aileron Province and the Alcurra dolerite into the Musgrave Province, predate the deposition of the Heavitree Formation and the Dean Quartzite. This is also true to the Tjauwata Group rift succession in the southwest dated at 1080–

1050 Ma (Edgoose 2012; Lindsay 1999). The completion of the deposition occurred at ca 820 Ma based on geochemical affinities in the overlying Bitter Springs Formation with mafic dykes of the Amata Dolerite in the Musgrave Province which showed a 800 Ma Sm-Nd isochron age (Zhao et al. 1994) and a ca 820 Ma U-Pb Baddeleyite age (Glikson et al. 1996). The provenance and maximum depositional age of the Heavitree Formation are not well constrained. Several studies revealed different results of possible source regions and ages (Edgoose 2012). Both, the Arunta Region and the Musgrave Province are contributing to the Amadeus Basin in variable degrees over time.

Here, we present new U-Pb and Hf data from nine samples of the Amadeus Basin Heavitree Formation to a) better constrain the age of the Heavitree Formation, b) investigate the spatial variation in provenance of the Heavitree Formation, and, c) compare with other 'Supersequence 1' quartzites from the wider Centralian Superbasin.

GEOLOGICAL SETTING

The Amadeus Basin and Centralian Superbasin

The Amadeus Basin is located at the centre of the Australian continent, covering an area of 170 000 km². It is a large and elongate intracratonic basin that extends 300 km north-south and 800 km east-west (Munson et al. 2012). The Amadeus Basin is mostly exposed in the Northern Territory and extends to the west in Western Australia (Edgoose 2012). Stratigraphically, the Amadeus Basin overlies the Musgrave Province basement in the south and the Aileron and Warumpi provinces in the north.

Sedimentation in the basin started at the Neoproterozoic and continued until Late Devonian/Early Carboniferous. During this geologic period, sedimentation was influenced by laterally migrating depocentres due to the ongoing processes of basin development and localized periods of contraction and extension (Munson et al. 2012). This influence resulted in the morphological features observed in the basin such as the central ridge. The Amadeus Basin experienced two major intracratonic orogenic events. The first orogenic event was the Petermann Orogeny that occurred in 580–530 Ma and the second event was the Alice Springs Orogeny during 450–350 Ma that formed the currently observed folding and dome structures (Munson et al. 2012). Furthermore, the Amadeus Basin formed part of the Neoproterozoic–Early Palaeozoic Centralian Superbasin and was contiguous with other, currently separated, basins in northern, central and southern Australia. Together with Officer, Ngalia, Georgina, Murraba, Wolfe and Victoria basins, the Amadeus Basin formed part of the Centralian A Superbasin (Munson et al. 2012). The formation of the Centralian Superbasin coincided with the NE–SW directed intracratonic extension across the Rodinia Supercontinent,

which eventually led to the break-up North America and Australia at ca 839 Ma, which is described as the Centralian 1 according to Walter and Veevers (2000). The Centralian 2 recorded a localized and renewed sedimentation related to 700–690 Ma Sturtian glaciation and the Centralian 3 was associated to the younger Elatina glaciation. Sedimentation of the Centralian A Superbasin a single extensive depositional system terminated by 580–530 Petermann Orogeny, which coincided with the final stages of the assembly of Gondwana (Munson et al. 2012). In fact, the Petermann Orogeny was characterized by the exhumation and uplift of the Musgrave Province that resulted in the separation of the Officer Basin from the other components of the superbasin. Following this orogenic event, the Amadeus Basin formed part of the Centralian B Superbasin. The superbasin was dismembered by the 450–350 Ma Alice Springs Orogeny through compressional deformation and sedimentation ceased in the mid-Carboniferous. Moreover, U-Pb dating of detrital zircon and Sm-Nd isotopic studies identified two dominant source regions in the Amadeus Basin and are the Musgrave Province in the south and the Arunta Region in the north (Munson et al. 2012).

The Heavitree Formation

The Heavitree Formation, previously named the Heavitree Quartzite, is the basal unit of the Amadeus Basin alongside with its equivalent the Dean Quartzite. They represent a widespread, sheet-like, uniform deposits. The Heavitree Formation and the Dean Quartzite are mostly exposed in the northern and southwestern margins of the current basin boundaries. Moreover, the characteristics of the formation imply abundant supply of sediment being deposited in high-energy shelf-like environments (Edgoose 2012). According to Lindsay (1993,1999), sedimentological and stratigraphic analysis revealed that these clastic layers formed from quartz sandstone sedimentation in

shallow, low-gradient ramp setting. Quartz clastic material was transported by heavily laden braided streams to the basin and eventually been dispersed in high-energy, shallow marine environment forming the extensive sheet-like sand bodies. The deposition of the Heavitree Formation occurs post the intrusion of the Stuart Pass and Alcurra dolerites into the underlying basement of the Aileron Province and the Musgrave Province respectively. It also postdates the intrusion of the Tjauwata Group rift succession in the southwest dated at 1080–1050 Ma (Edgoose 2012). According to the geochemical affinities of spilites at the base of the upper member of the Bitter Springs Formation with mafic dykes of the Amata Dolerite in the Musgrave Province, the deposition of the Heavitree Formation terminated by ca.820 Ma as the geochemical affinities resulted in a ca 800 Ma Sm-Nd isochron age (Zhao et al. 1996) and a ca 820 Ma U-Pb baddeleyite age (Glikson et al. 1996). Different studies revealed different source regions of sediments for the Heavitree Formation. Zhao et al. 1992 have provided an age range indicating the Arunta Region as the dominant source. On the other hand, Maidment et al. (2005) provided the youngest grain at 1120 Ma, which is most probably related to the Musgrave Province. To a reasonable extent, both the Arunta Region and the Musgrave Province contributed to sediments in the Heavitree Formation (Edgoose 2012).

METHODS

U-Pb zircon geochronology

A total of eight field samples and one drill core sample were collected from various locations Figure 1. Zircons were extracted from crushed rocks using standard strong magnet, Frantz (1.00 AMP and 1.60 AMP) and heavy liquids techniques (Howard et al. 2009). Detrital zircons were then hand-picked and mounted in a non-reactive epoxy resin without any preference to size, shape or colour. The zircon mounts were then polished to expose the minerals to the surface and sent to Adelaide Microscopy, the University of Adelaide, to get carbon coated. Cathodoluminescence (CL) images of the mounts were then captured using FEI Quanta 600 Scanning Electron Microscope (SEM) with attached Gatan CL Detector to help identifying internal structures of the zircons.

U–Pb isotopic data were collected using Laser Ablation Inductively Coupled Plasma Mass Spectrometry (LA-ICP-MS) in Adelaide Microscopy. A 30 µm spot size, 5.50 J/cm² fluence and 5 Hz repetition rate were used for the analysis. Instrumental fractionation was corrected using the zircon standard GEMOC GJ-1 with ²⁰⁷Pb/²⁰⁶Pb age of 607.7 ± 4.3 Ma, ²⁰⁶Pb/²³⁸U age of 600.7 ± 1.1 Ma and ²⁰⁷Pb/²³⁵U age of 602.0 ± 1.0 Ma (Jackson et al. 2004), and accuracy was controlled using Plešovice zircon standard with ²⁰⁶Pb/²³⁸U age of 337.13 ± 0.37 Ma (Slama et al. 2008). Data were reduced using Iolite (Paton et al., 2011) and plotted using the Excel add-in Isoplot (Ludwig, 2003). Zircon U-Pb discordance was calculated by dividing the ²⁰⁶Pb/²³⁸U age by the ²⁰⁷Pb/²⁰⁶Pb age and multiplying by 100. Only analyses that are under 5% discordant were used and are shown in the U-Pb concordia Wetherill plots and

discussed further (Figure 2). In this study, for the best estimate of the ‘age’ of the detrital grains we chose to use the $^{206}\text{Pb}/^{238}\text{U}$ age for zircons younger than 1.2 Ga. For zircons older than 1.2 Ga, the more precise of the ages was used. However, if both ages, $^{206}\text{Pb}/^{238}\text{U}$ age and $^{207}\text{Pb}/^{206}\text{Pb}$ age, had the same error value then $^{207}\text{Pb}/^{206}\text{Pb}$ age was considered. In determining the maximum depositional age, we followed Spencer and Kikland (2016) in using a single grain ages due to there being no *priori* reason that any two zircon grains should have the same age in any sandstone.

Multidimensional Scaling (MDS) is used in this study. It is a provenance analysis technique proposed by Vermeesch (2013) to compare sample similarities. This technique is conducted on the Provenance package in R (Vermeesch 2013). Using the Kolmogorov-Smirnov (K-S) test, the dissimilarity (D-value) between two age distributions can be quantified. The D-value is then used to generate n-dimensional matrix (where ‘n’ is the number of samples being compared) and projects this matrix in a two-dimensional plane, which is the MDS plot. The MDS plot reveals the similarity or dissimilarity among data sets in the proximity of the points to each other. The most similar sample plotted closest together and connected by a solid line (the second most similar samples are connected by a dotted line). This method was used to test and compare the collected samples with possible provenance data.

Lu-Hf isotopes determination

Analytical methods for zircon Hf isotope determination were based upon Payne et al. (2013) and Griffin et al. (2006). Analysis undertaken using New Wave UP-193 Laser attached to a Thermo-Scientific Neptune Multi-Collector ICP-MS at the University of Adelaide. A size of 50 μm used in analysis spots that was reduced to of 30 μm for small grains. Data reduction was implemented using a macro-driven Hf isotope data reduction Excel (Microsoft 2007) spreadsheet, Hf TRAX, coded by corresponding author (Payne et al. 2013). Results were normalised to $^{179}\text{Hf}/^{177}\text{Hf}=0.7325$, using an exponential correction for mass bias. Standards were analysed before and during analysis of unknowns to check instrument performance and stability. The measured $^{176}\text{Lu}/^{177}\text{Hf}$ ratios of the zircons have been used to calculate initial $^{176}\text{Hf}/^{177}\text{Hf}$ ratios. These age corrections are very small, and the typical uncertainty on a single analysis of $^{176}\text{Lu}/^{177}\text{Hf}$ (+1%) contributes and uncertainty of $<0.05 \epsilon_{\text{Hf}}$ unit (Payne et al. 2013). Twenty five Mud Tank standards were analysed giving an average value of 0.282512 ± 0.00001 .

RESULTS

U-Pb isotopic data

U—Pb geochronology was undertaken on seven out of nine samples of the Heavitree Formation Figure 1. Samples HQ-02 and HQ-07 did not contain any zircon grains. These data are plotted on Wetherill Concordia plots (Figure 2). All age uncertainties are quoted at a 2σ level. Due to the high number of concordant analyses

obtained, a 5% concordance cut-off has been used to quote the ages. Sample descriptions are summarised in Table 1.



Figure 1: Collected samples locations in the north of the Amadeus Basin. Two Heavitree Formation locations added after Normington et al. (2016) and Kositein (2014). Modified after Edgoose (2012).

HQ-01

Zircons in HQ-01 are within the size of 100 μm to 300 μm . Zircons are mostly subhedral with some prismatic and fractured grains. CL images of these grains reveal oscillatory-zones and thickened banding internal structure. A total of 109 zircons were

analysed and 90 analyses fall within 5% concordance (Figure 2a) forming a broad range from 3247 Ma to 1139 Ma. This range formed three age peaks clustering at ca. 1147 Ma, 1614 Ma, and 2000 Ma with two Archean ages at 2667 ± 42 Ma and 3247 ± 48 Ma. Five grains that form the youngest population yielded a weighted mean age of 1148 ± 11 Ma with a MSWD of 1.12. The youngest concordant zircon analysis yielded a $^{206}\text{Pb}/^{238}\text{U}$ age of 1139 ± 30 Ma, interpreted to best represent the maximum depositional age for this sample.

HQ-03

Sample HQ-03 yielded the finest zircon grain sizes ($<100\mu\text{m}$) with few coarser grains. They range from subhedral to anhedral structures with prismatic to more rounded shapes. Internal structures of the zircons seen in CL images vary within the sample. Several zircons show oscillatory-zones and few grains contain high luminescent rims. 95 zircon grains were analysed and 53 analyses are within 5% concordance (Figure 2b). Sample HQ-03 yielded ages ranging from 2330 Ma to 1064 Ma, with two major peaks at ca. 1550 Ma and 1605 Ma as well as two minor peaks at ca. 1130 Ma and 1790 Ma. It also yielded two Palaeoproterozoic analyses at 1943 ± 48 Ma and 2330 ± 49 Ma. Three grains of the youngest population yield a weighted average age at ca. 1143 ± 53 Ma with a MSWD value of 2.8. Statistically, the MSWD value is not within the valid range for a single population and therefore those grains are probably sourcing multiple regions. The youngest concordant zircon analysis yielded a $^{206}\text{Pb}/^{238}\text{U}$ age of 1064 ± 24 Ma and hence maximum depositional age for this sample.

HQ-04

The zircon grain sizes in HQ-04 range from 100 μm to 300 μm . The majority of the zircons have a subhedral structures with a relatively prismatic shape. Internal structures seen in CL images vary from oscillatory-zoned cores to thin, bright luminescent rims. 85 out of 169 zircons analysed are within 5% concordance (Figure 2c). They range in age from 2571 Ma to 1078 Ma. These ages are mainly clustering at ca. 1590 Ma with two minor peaks at ca. 1144 Ma and 1791 Ma with one Archean age at 2571 ± 60 Ma. The youngest population (3 grains) yield a weighted average age of 1141 ± 15 Ma with a MSWD value of 1.2. The youngest zircon grain yielded a $^{206}\text{Pb}/^{238}\text{U}$ age of 1078 ± 34 and therefore the maximum depositional age for this sample.

HQ-05

Sample HQ-05 yield zircon grain sizes in the range of 100-300 μm . Most grains are subhedral and rounded in shape. Several internal structures observed in CL images including thickened banding, oscillatory zoning and fir-tree zoning. A total of 227 were analysed and 153 are within 5% concordance (Figure 2d) ranging in age from 2924 Ma to 1029 Ma. There are two major age peaks clustering at ca. 1152 Ma and ca. 1742 Ma with two minor peaks at ca. 1458 Ma and 1578 Ma. Three Early to Mid-Archean grains show a spread of ages between 2924 and 2708 Ma. The youngest population with four grains show a weighted average age of 1087 ± 24 Ma with a MSWD value of 1.9. The youngest zircon analysed yielded a $^{206}\text{Pb}/^{238}\text{U}$ age of 1029 ± 21 Ma which is the maximum depositional age for this sample.

HQ-06

Sample HQ-06 yield zircons within 80-300 μm in size. They vary from subhedral to anhedral structures and elongate to rounded shapes. Zircons in this sample appear in CL images with oscillatory-zones and thickened banding with occasional thin luminescent rims. A total of 117 grains were analysed and 82 analyses are within 5% concordance (Figure 2e). They range in age from 2426 Ma to 1113 Ma. These ages mainly cluster at age peak around ca. 1602 Ma and two minor peaks at ca. 1134 Ma and 1786 Ma with one Palaeoproterozoic grain at 2426 ± 49 Ma. The youngest population with five grains yielded a weighted average age of 1136 ± 22 Ma with MSWD of 1.9. The youngest zircon grain analysis yielded a $^{206}\text{Pb}/^{238}\text{U}$ age of 1113 ± 27 Ma representing the maximum depositional age for this sample.

HQ-08

Zircons in HQ-08 are in the size range of 80-250 μm . Most zircon grains are subhedral and fractured and have prismatic to rounded shapes. CL images of these zircons reveal oscillatory-zoned and fir-tree zone internal textures. 106 grains were analysed and 78 analyses are within 5% concordance (Figure 2f). The ages in HQ-08 range from 2452 Ma to 1142 Ma mainly clustering at age peak of ca. 1760 Ma. This age spread also clusters at minor age peaks at ca. 1150 and 1590 Ma with one Archean grain at 2452 ± 42 Ma. The youngest zircon grain yielded a $^{206}\text{Pb}/^{238}\text{U}$ age on 1142 ± 27 Ma and therefore the maximum depositional age for sample HQ-08.

BL-002

Sample BL-002 consist of 80-260 μm zircon grains. These grains are mostly subhedral and have rounded shapes. Oscillatory-zones and thickened banding are observed in CL images. A total of 79 grains were analysed and 48 analyses fall within 5% concordance (Figure 2g). Ages in sample BL-002 range from 1969 Ma to 1096 Ma and mostly clustering at age peak ca. 1564 Ma. The spread of ages also clusters in two minor peak at ca. 1135 Ma and 1735 Ma with one Palaeoproterozoic grain at 1969 ± 38 Ma. Three grains forming the youngest population yielded a weighted average age of 1129 ± 38 Ma with 1.5 MSWD value. The maximum depositional age in this sample is constrained by the youngest zircon grain yielding a $^{206}\text{Pb}/^{238}\text{U}$ age of 1096 ± 24 Ma.

Sample	Description	GPS coordinates	Location
HQ-01	Medium grained quartz arenite	23°43'35.42" S 133°51'59.05" E	Heavitree Gap
HQ-02	Fine grained mudstone	23°38'15.29" S 132°43'57.72" E	Ormiston Gorge
HQ-03	Muscovite rich, fine grained mudstone	23°38'15.29" S 132°43'57.72" E	Ormiston Gorge
HQ-04	Medium grained quartz arenite	23°38'11.44" S 132°43'55.57" E	Ormiston Gorge
HQ-05	Medium grained quartz arenite	23°37'27.43" S 132°44'15.0" E	Ormiston Gorge
HQ-06	Fine grained quartz arenite	23°46'37.66" S 133°04'26.08" E	Ellery Creek
HQ-07	Fine grained carbonate (Gillen Formation)	23°47'34.4" S 133°04'24.12" E	Ellery Creek
HQ-08	Medium grained quartz arenite	23°43'37" S 133°51'55" E	Heavitree Gap
BL-002	Medium grained sandstone	23°30'4.03" S 134°44'38.91" E	BL-002 drillhole

Table 1: Collected samples descriptions and locations.

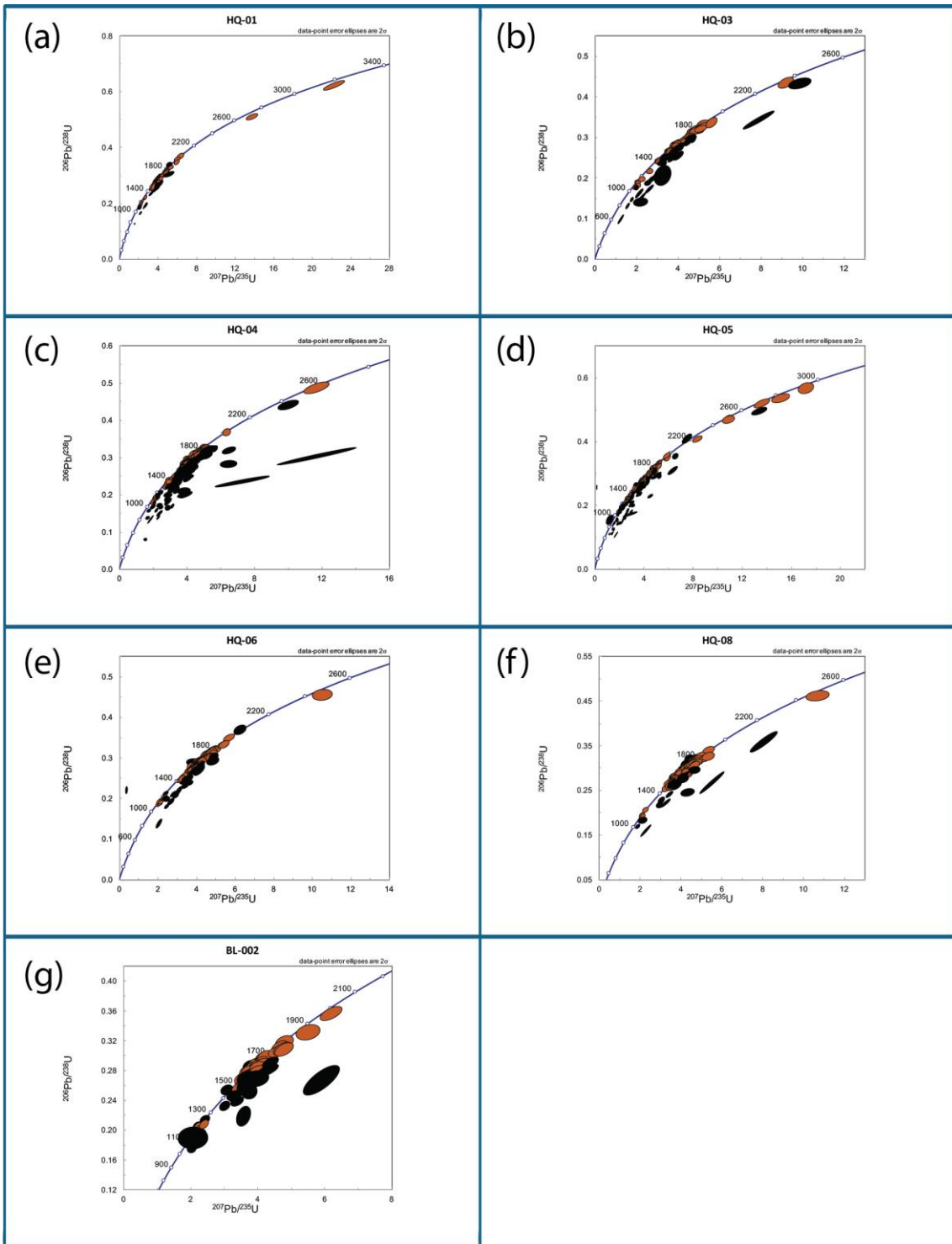


Figure 2: Wetherill Concordia plots of all samples analysed.

Lu-Hf isotopic data

Lu–Hf isotopes in zircon have been conducted on six samples. Data are presented as $\epsilon\text{Hf}(t)$ versus U–Pb age data (Figure 3). Uncertainties on Lu–Hf data are quoted at the 2σ level.

HQ-01

A total of nineteen analyses for Lu-Hf isotopes were undertaken (Figure 3a). The youngest population (1141–1306 Ma) have a large spread in $\epsilon\text{Hf}(t)$ data of (-10.54– -44.90) and therefore evolved. The data of ages between ca. 1500 Ma and 1950 Ma have $\epsilon\text{Hf}(t)$ values between -10.63 and +16.31 suggesting a multiple, evolved and juvenile, sources. Three grains of ages older than ca. 2000 Ma yielded $\epsilon\text{Hf}(t)$ values between +8.63 and +46.69 suggesting a considerably juvenile source.

HQ-04

Thirty four zircon grains were analysed in sample HQ-04 (Figure 3b). The youngest group of zircons with ages from 1097 Ma to 1450 Ma yield $\epsilon\text{Hf}(t)$ between +3.37 to +8.30 therefore dominantly sourced from a juvenile source. In the age range between ca. 1500 Ma to 1800 Ma, $\epsilon\text{Hf}(t)$ noticeably varies from dominantly positive (+2.26–+9.20) in younger grains to dominantly negative (-7.79– -0.44) in older grains suggesting a change from a juvenile to a more evolved source. A single grain at 2571 Ma with an $\epsilon\text{Hf}(t)$ of -0.68 suggesting an evolved source.

HQ-05

A total of thirty grains were analysed in sample HQ-05 (Figure 3c). The $\epsilon\text{Hf}(t)$ values shows a spread across all ages. The age range between ca. 1050 Ma and 1200 Ma have $\epsilon\text{Hf}(t)$ values between -13.01—+6.24 suggesting multiple, evolved and juvenile, sources. The data between ca. 1400 Ma and 2000 Ma range in $\epsilon\text{Hf}(t)$ values between -7.59 and +8.23, also suggesting a multiple source areas. Three grains of age older than ca. 2400 Ma preserve more juvenile ϵHf signatures (+0.34—+4.08).

HQ-06

In sample HQ-06, twenty zircon grains were analysed (Figure 3d). The three youngest grains yielding ages of 1113 Ma, 1137 Ma and 1200 Ma, have $\epsilon\text{Hf}(t)$ values of +0.06, -6.22 and -10.76 respectively. Therefore, the youngest grains is sourcing a juvenile source whereas the other two grains are sourcing more evolved magmas. In the age range between ca. 1400 Ma and 1800 Ma, $\epsilon\text{Hf}(t)$ values fall in the range of -6.95 and +6.09 and therefore sourcing evolved and juvenile sources. A single grain with 1939 Ma age preserve a juvenile source with ϵHf value of 1.46.

HQ-08

A total of twenty six zircons were analysed in sample HQ-08 (Figure 3e). The two youngest grains, ca. 1152 Ma and 1219 Ma, have $\epsilon\text{Hf}(t)$ of -12.05 and +0.70 respectively. Hence the former grain is sourcing an evolved source and the latter is sourcing a juvenile source. Grains of age between ca. 1450 Ma and 1900 Ma preserve $\epsilon\text{Hf}(t)$ values between -25.56 and +10.44 and therefore sourcing multiple regions. A single grain of age ca. 2452 Ma preserve a considerably juvenile source of $\epsilon\text{Hf}(t)$ value of 30.44.

BL-002

Sixteen zircon grains were analysed in sample BL-002 (Figure 3f). The two youngest grains, ca. 1096 Ma and 1139 Ma, preserve $\epsilon\text{Hf}(t)$ values of +2.67 and -2.60 suggesting different source characteristics. Two grains, ca. 1203 Ma and 1225 Ma, preserve an evolved source regions with values 2.30 and 0.80 respectively. The values of $\epsilon\text{Hf}(t)$ varies between -6.04 and +5.34 in ages between ca. 1450 Ma and 1850 Ma. This suggest a multiple source regions are preserved in these zircons. A single grain, ca. 1969 Ma, preserve a juvenile source $\epsilon\text{Hf}(t)$ value of 12.96.

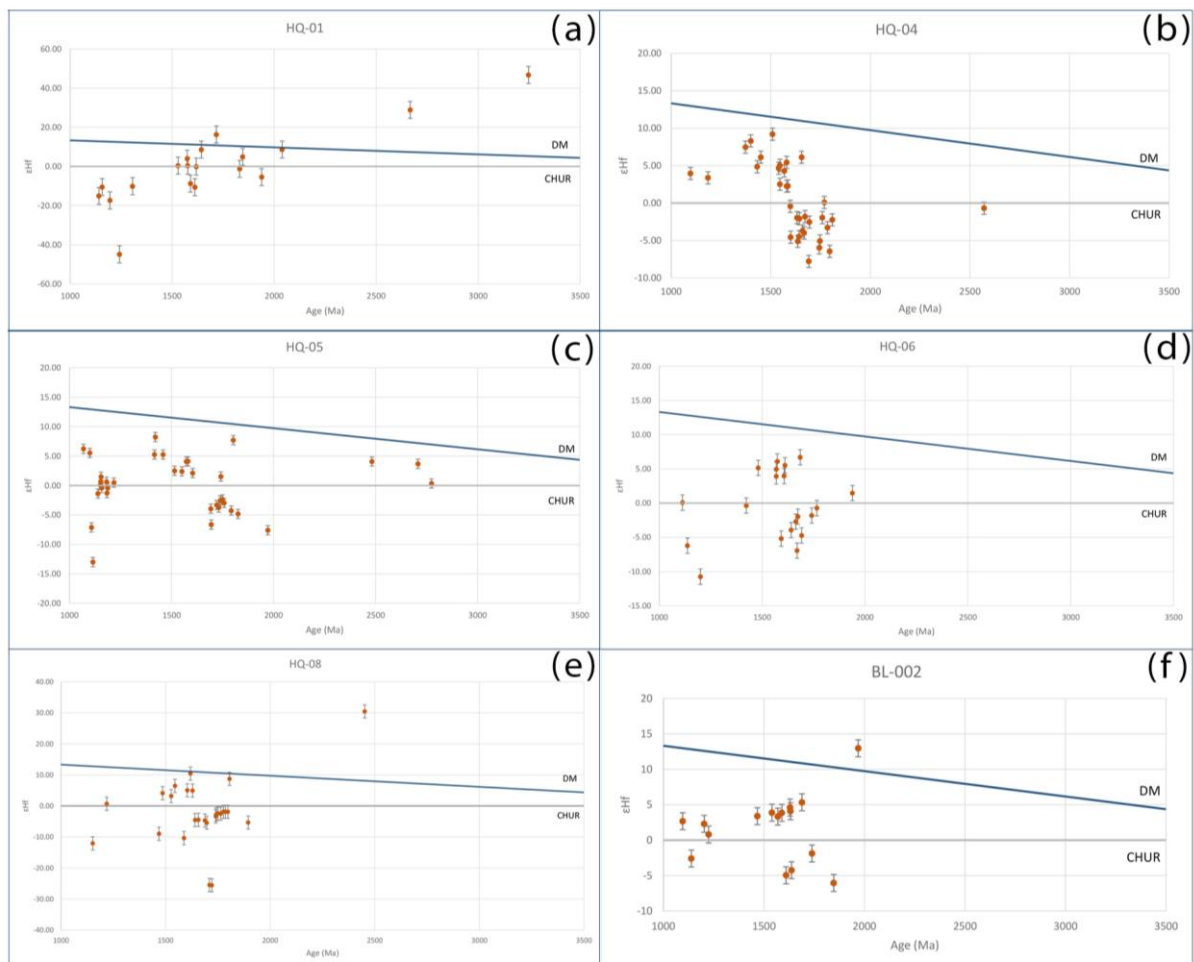


Figure 3: $\epsilon\text{Hf}(t)$ value of samples analysed.

Rare-Earth-Element analysis in zircon

HQ-01

The pattern of REE in samples shows a negative Eu anomalies ($(Eu/Eu^*)_{N=}$ 0.056—0.52) and positive Ce anomalies ($(Ce/Ce^*)_{N=}$ 1.2—256).. The REE pattern also reveals enrichment in HREE ($(Yb/Sm)_{N=}$ 18—177) with one (ca. 1195 Ma) extreme $(Yb/Sm)_{N=}$ value of 1552. All REE patterns observed retain similar slopes except one grain (ca. 1794 Ma) that have a relatively flat pattern in LREE and hence possibly sourced from different magma.

HQ-03

Sample HQ-03 preserve REE with negative Eu anomalies ($(Eu/Eu^*)_{N=}$ 0.03—0.5) and positive Ce anomalies ($(Ce/Ce^*)_{N=}$ 1.14—87). The HREE ($(Yb/Sm)_{N=}$ 21—141) values show moderate to high enrichments of these elements. Two zircon grains of age ca. 1550 Ma and 1597 Ma have enrichment in LREE values.

HQ-04

Sample HQ-04 REE pattern marks a negative Eu anomalies ($(Eu/Eu^*)_{N=}$ 0.04—0.6) and positive Ce anomalies ($(Ce/Ce^*)_{N=}$ 1.2—124). It also preserve moderate to high HREE enrichment ($(Yb/Sm)_{N=}$ 29—441) which suggests the low probability of garnet growth with zircon in the parental magma. The REE pattern of all analyses appears similar except for two analyses (ca. 1642 Ma and 1759 Ma). Both analyses have enrichment in LREE.

HQ-05

The pattern of REE in sample HQ-05 preserves negative Eu anomalies ($(\text{Eu}/\text{Eu}^*)_{\text{N}} = 0.023\text{—}0.63$) and positive Ce anomalies ($(\text{Ce}/\text{Ce}^*)_{\text{N}} = 1.1\text{—}141$). It also shows low to high HREE enrichment ($(\text{Yb}/\text{Sm})_{\text{N}} = 9.4\text{—}137$). These values suggest the possibility of zircon growth with garnet presence in the magma. Several grains in the analysis (ca. 1421 Ma, 1535 Ma, 1573 Ma, 1693 Ma, 1719 Ma and 2222Ma) have a relatively flat LREE pattern.

HQ-06

In sample HQ-06, negative Eu anomalies ($(\text{Eu}/\text{Eu}^*)_{\text{N}} = 0.023\text{—}0.50$) and positive Ce anomalies ($(\text{Ce}/\text{Ce}^*)_{\text{N}} = 2.7\text{—}119$) are evident. The level of HREE in sample HQ-06 varies from relatively moderate to high values ($(\text{Yb}/\text{Sm})_{\text{N}} = 26\text{—}377$). The REE pattern observed behave similarly in all grains analysed with, however, different magnitudes.

HQ-08

Sample HQ-08 REE patterns show negative Eu anomalies ($(\text{Eu}/\text{Eu}^*)_{\text{N}} = 0.021\text{—}0.50$) and positive Ce anomalies ($(\text{Ce}/\text{Ce}^*)_{\text{N}} = 1.6\text{—}140$). The HREE trend varies from relatively flat to steep ($(\text{Yb}/\text{Sm})_{\text{N}} = 16\text{—}187$). This indicates to the possibility of zircon growth with competition with minerals such as garnet that preserves HREE. Three analyses (ca. 1545 Ma, 1585 Ma and 1649 Ma) in sample HQ-08 have enrichment in LREE patterns.

BL-002

The REE pattern in sample BL-002 marks negative Eu anomalies ($(Eu/Eu^*)_N = 0.051—0.47$) and positive Ce anomalies ($(Ce/Ce^*)_N = 1.6—115$). It also shows enrichment in HREE ($(Yb/Sm)_N = 25—161$) which suggest that zircon did not grow in competition with garnet. All analysed grains shows similar REE pattern except for one grain of age ca. 1632 Ma that have relatively flat LREE pattern.

All samples analysed appear to have similar trends. They all preserve a negative Eu anomaly and positive Ce anomaly. This indicates that these zircon evolved in magma with plagioclase present and have high oxidation state. All zircon show varying degree of enrichment in HREE. The older populations have relatively high HREE than younger populations. Few analysed grains show enrichment in LREE. This would indicate a different magma source or that these analysed spots are metamict or have inclusions with high LREE levels (Belousova 2002).

DISCUSSION

Maximum Deposition constraints

Based on the geochemical affinities of spilites in the overlying Bitter Springs Formation with mafic dykes of the Amata Dolerite in the Musgrave Province, the deposition of the Heavitree Formation completed by 820 Ma (Edgoose 2013). These gave a ca. 800 Ma Sm-Nd isochron age and a ca. 820 Ma U-Pb baddeleyite age and hence constraining the minimum time of deposition. The deposition of the Heavitree Formation post-dates dolerite dykes intruding the basement. One of those is the widespread Alcurra Dolerite in the Musgrave Province that yields a 1054 ± 14 Ma Rb-

Sr age and 1090 ± 32 Sm-Nd age providing a maximum age constraint for the Heavitree Formation (Edgoose 2013). Several detrital zircon studies conducted on the Heavitree formation provided different maximum deposition ages. In Hollis et al. (2013), the youngest detrital zircon grain yielded a $^{207}\text{Pb}/^{206}\text{Pb}$ age of 1198 ± 24 Ma, whereas in Kositcin et al. (2014) study the youngest zircon age obtained was 1050 ± 10 Ma. The most recent study by Normington et al. (2016) provided a maximum age of deposition of 1073 ± 12 Ma. In this research, seven samples of the Heavitree Formation were analysed. A single, youngest, 96% concordant with a $^{206}\text{Pb}/^{238}\text{U}$ age of 1029 ± 21 Ma constitutes a maximum age constraint for the time of deposition for the Heavitree Formation. This age overlaps (in 2 sigma) with youngest zircon analysis from Kositcin et al (2014).

Spatial and temporal variance

The seven samples used in this research were collected from various locations along the MacDonnell Ranges in Northern Territory with one drill-core sample about 100 km east of Alice Springs. Samples HQ-08 and HQ-05, from the east and west respectively, represent the older succession of the Heavitree Formation. Both samples share similar age peaks (Figure 4) clustering around 1800—1700 Ma, 1650—1550 Ma and 1200-1100 Ma. However, sample HQ-05 have more zircon grains of the younger ages around 1500—1400 Ma and even more around 1200—1100 Ma. Both samples plot distant from each other in MDS plots indicating that they less similar to each other (Figure 6). As both samples are spatially spread, around 150 km apart, the variance in age clusters would indicate a dominant younger source in the west and older source in the east. All other samples were collected from the upper succession of the Heavitree Formation. They all show similar age distribution and a main age cluster around 1650—

1550 Ma (Figure 4). There is no significant change observed in age distribution from east to west and they all plot closely in MDS plots (Figure 6). Therefore, a source of age 1650—1550 Ma is contributing mostly to the younger successions of the Heavitree Formation.

Additional samples of Heavitree Formation after Kositsin et al (2014) and Normington et al. (2016) were used in the comparison (Figure 4 and 6). These samples are located in Limbla area, which is further east to the location of samples used in this study. They show similar age distributions (Figure 4 and 6) to sample HQ-08 enhancing the argument that older sources are contributing more to early successions of the Heavitree Formation in the east.

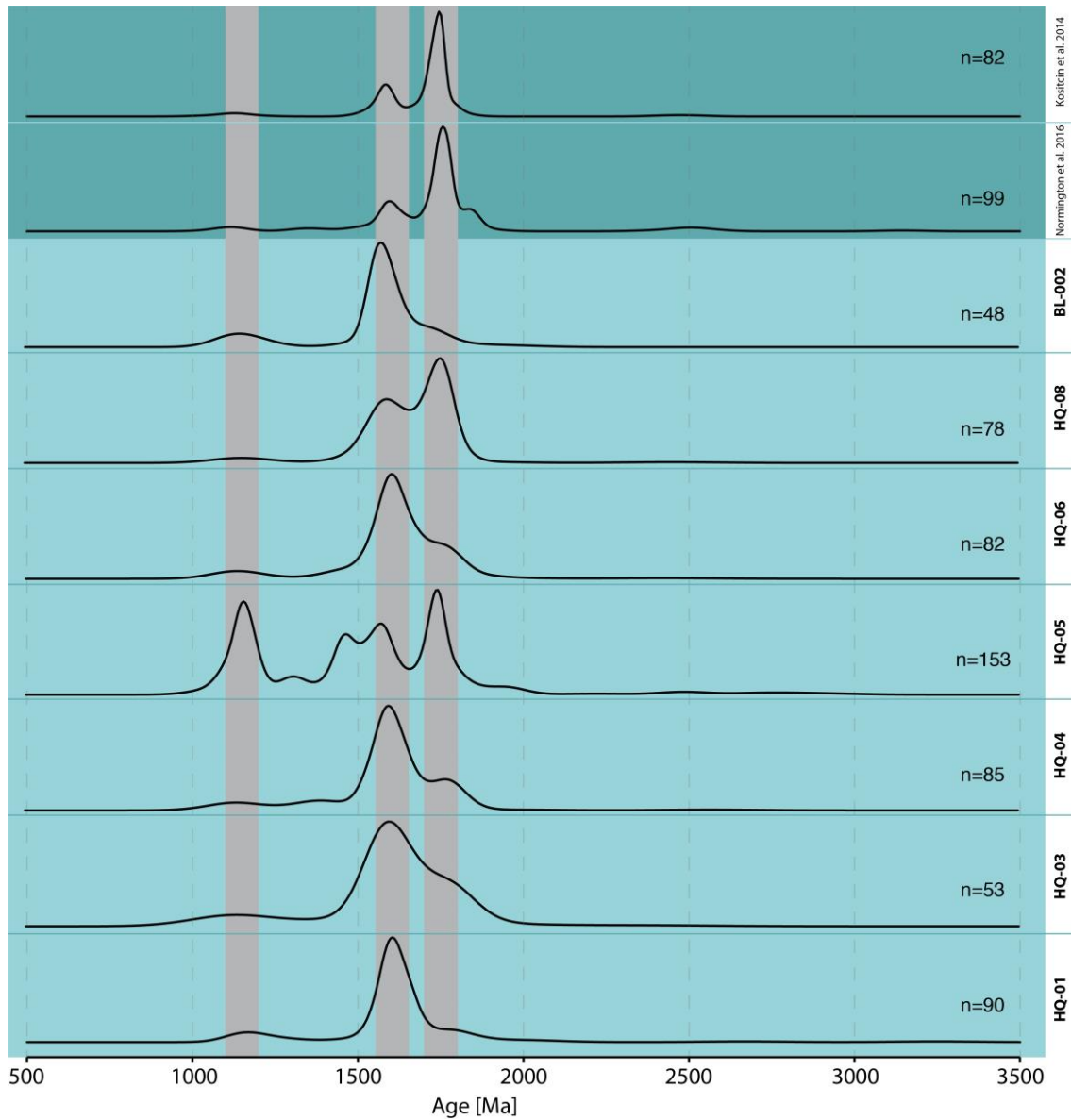


Figure 4: Samples comparison in KDE. Additional Heavitree Formation obtained after Normington et al. (2016) and Kositcin et al (2014).

Heavitree Formation equivalent formations

The Heavitree Formation along with other basal Neoproterozoic successions are interpreted to form the Centralian Superbasin. The superbasin is contiguous with Adelaide Fold Belt (Munson et al. 2012). These basal units include the Munyu Sandstone in Murraba Basin, Jamison Sandstone in Beetaloo Sub-basin, Jasper Gorge Sandstone in Victoria Basin and the Paralana Quartzite in the Adelaide Fold Belt.

Additional published data of these units are used to aid the comparison with the the Heavitree Formation after Job (2013), Yang et al. (2018), Carson (2013) and Hollis et al. (2013). The age distribution of all these sandstones shares an age cluster around 1650—1550 Ma (figure KDE). Munyu sandstone, Paralana Quartzite and Upper Jamison Sandstone also share another peak at ca. 1200 Ma. This is also observed on the MDS plot (Figure 6), all three formations plot close to each other suggesting a similar age distributions with minor contribution from other sources in the Paralana Quartzite. All the equivalent units plot close to the Heavitree Formation on the MDS plot suggesting existing similarities in overall age distribution of these formations. Hence, this supports the concept of the Centralian Superbasin and aids in understanding the equivalent sandstones of the Heavitree Formation.

Provenance Analysis

In this study, MDS and KDE plots together with ϵHf against age plots are used in conjunction to reduce the inaccuracy caused by MDS and enhance the spatial analysis (Figure 5 and 6). Published igneous zircon U-Pb ages (LA-ICP-MS and SHRIMP data) from potential source regions that surround the Amadeus Basin were also collected and used in MDS, KDE and ϵHf analysis. These potential source regions are the Warumpi Province and Aileron Province to the north, the Mount Isa Province (Eastern Fold Belt, Western Fold Belt and Kathleen Fold Belt) to the northeast and the Musgrave Province to the south.

In figure (Figure 4 and 5), samples from older succession of Heavitree Formation (HQ-05 and HQ-08) share similar age clusters to the Aileron Province and Eastern Fold Belt at ca. 1700 Ma and 1600 Ma. Both samples also share another age

peak at ca. 1200 Ma equivalent to the Musgrave Province with relatively higher proportion in sample HQ-05 than HQ-08. The ϵ_{Hf} values at ca. 1200 Ma for both samples plot in the Musgrave Province range. In ca. 1600 Ma and 1700 Ma populations, ϵ_{Hf} values from both samples plot in the Eastern Fold Belt and Aileron Province ranges respectively. No age or ϵ_{Hf} values similarities observed between these samples and Warumpi Province, the Western Fold Belt and Kathleen Fold Belt. The difference in sources between those samples is enhanced by MDS plots (Figure 6) as sample HQ-05 plots closer to the Musgrave Province and sample HQ-08 plots closer to the Aileron Province and the Eastern Fold Belt. Sample HQ-05 is located in the west indicating that sediments derived from the Musgrave Province are dominantly distributed in the western side of the basin in older succession of Heavitree Formation and the Aileron Province and the Eastern Fold Belt contributing more to the east.

Samples HQ-01, BL-002, HQ-06, HQ-03 and HQ-04 represent the upper succession of the Heavitree Formation. They all share similar age clusters in KDE (Figure 4 and 5) mainly at ca. 1600 Ma and minor peaks at ca. 1200 Ma and 1700 Ma. The age peak at ca. 1600 Ma correlates with the Eastern Fold Belt age and the other peaks at ca. 1200 Ma and 1700 Ma are more related to the Musgrave Province and the Aileron Province respectively. The ϵ_{Hf} values of ca. 1200 Ma age cluster for all samples plot in the Musgrave Province range. The age population at ca. 1600 Ma have two ϵ_{Hf} clusters, one is plotting in the Eastern Fold Belt range and the other is clustering in the Aileron Province range. All ϵ_{Hf} of age ca. 1700 Ma cluster in the Aileron Province range. In figure (Figure 6), these samples plot closer to the Eastern Fold Belt and Aileron Province revealing similarities in age distribution. The samples are spatially distributed from east to west across the Amadeus Basin and show no

noticeable variation in age clusters. No age similarities observed between these samples and Warumpi Province, the Western Fold Belt and Kathleen Fold Belt. This suggest that younger successions of the Heavitree Formation are dominantly sourced from the Eastern Fold Belt and the Aileron Province.

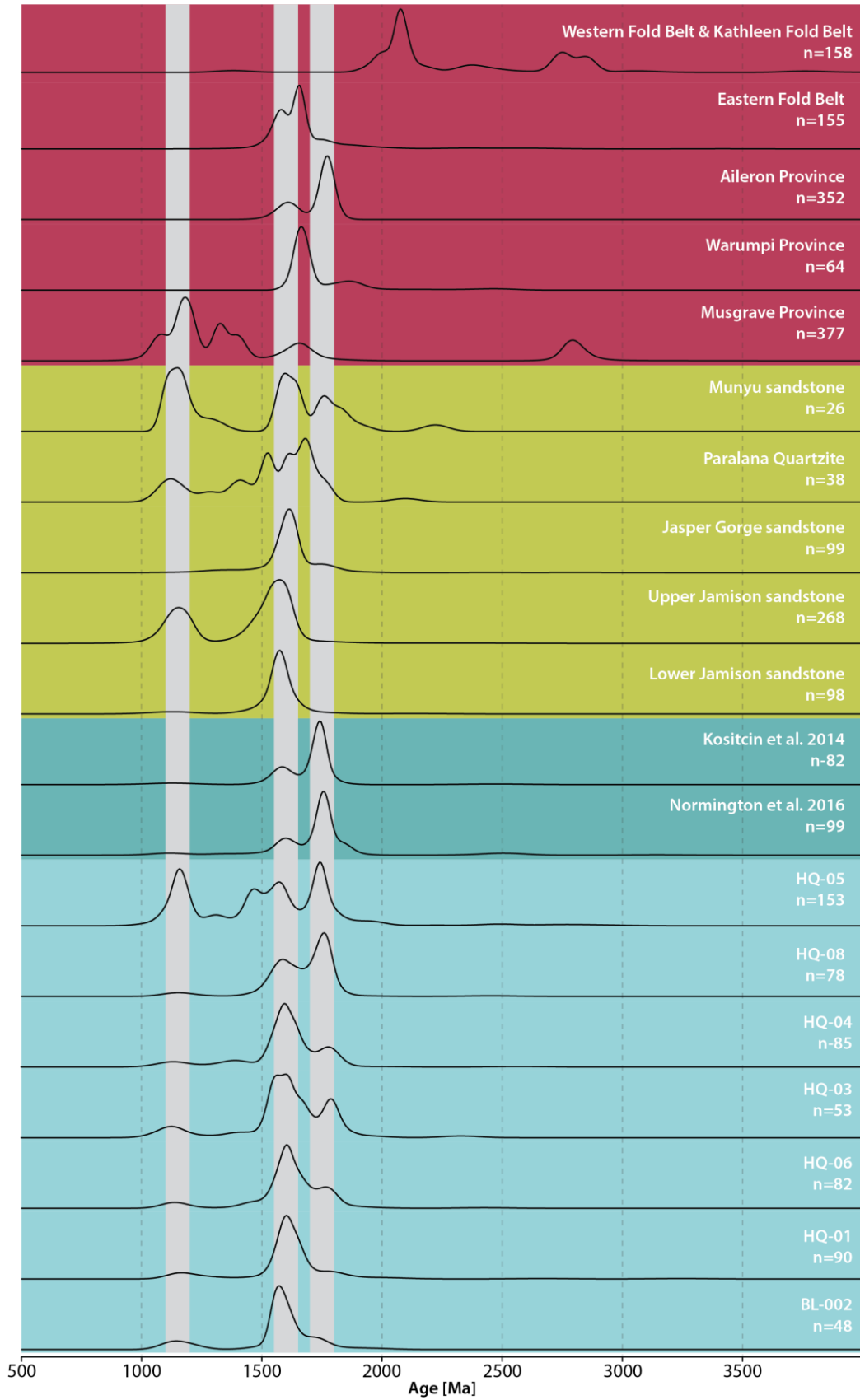


Figure 5: KDE plot off all samples collected, Heavitree Formation equivalent sandstones and potential source regions.

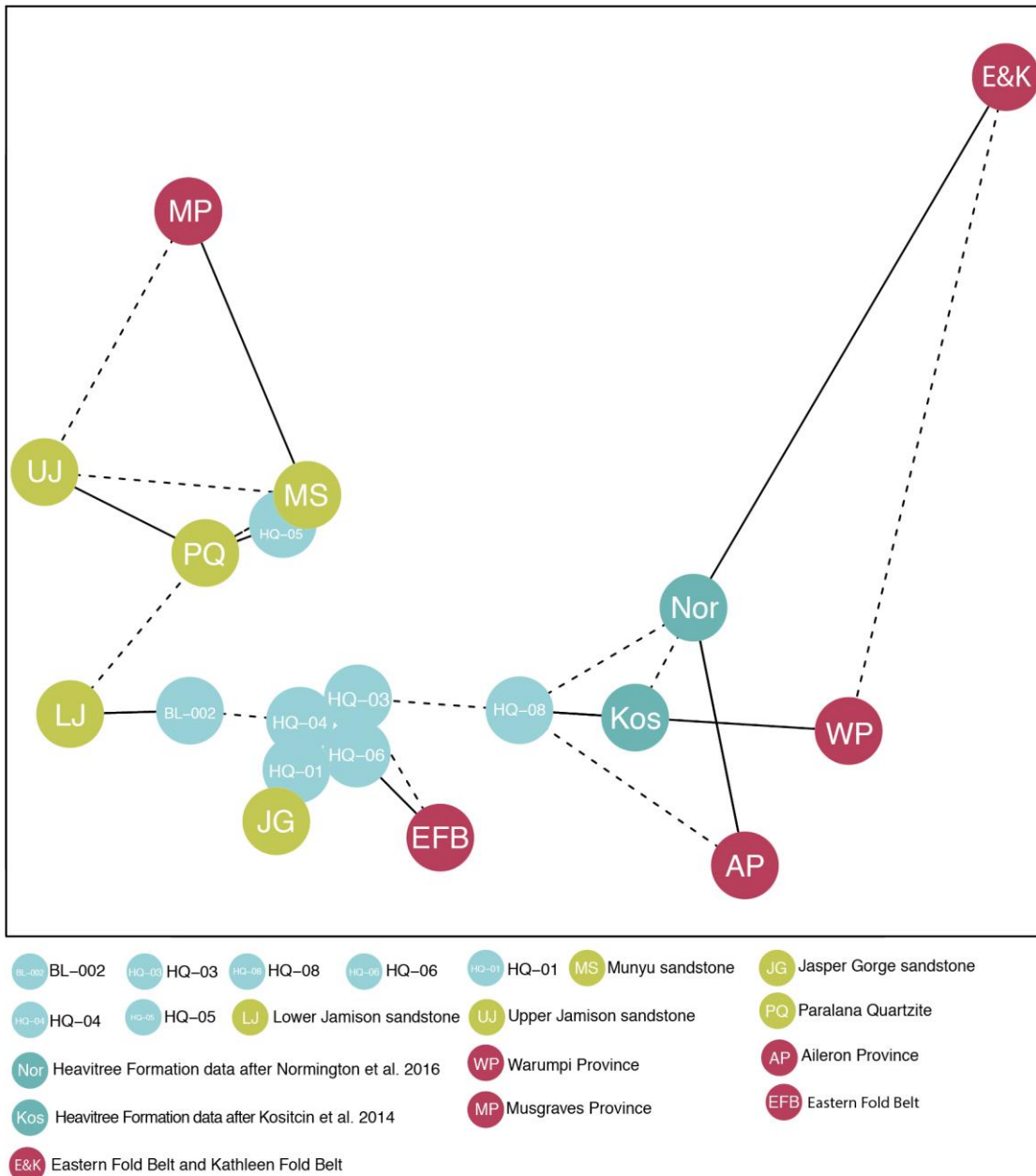


Figure 6: MDS of all samples collected, Heavtree Formation equivalents and potential source regions.

CONCLUSIONS

New detrital zircon data are presented in this research providing age constraints on the age and provenance of the Heavitree Formation. The use of Multidimensional Scaling (MDS) and Kernel Distribution Estimates (KDE) in conjunction with ϵHf values improved our understanding of age populations and source regions. The main conclusions of this research are:

- 1) The maximum depositional age of the Heavitree Formation is constrained at 1029 ± 21 Ma. No ages younger than 1000 Ma were obtained. The Heavitree Formation is now constrained to be deposited between 1008 Ma and 820 Ma.
- 2) Although spatial variance exists, the Heavitree Formation share similar age distributions and sources with the other Neoproterozoic basal units of the Centralian Superbasin. The data acquired in this research supports the concept of the superbasin and suggests that other Neoproterozoic sandstones not investigated in this research may have similar age distributions and sources and hence formed a single, extensive intracratonic basin.
- 3) Temporal and spatial variance of sources exists across the succession of the Heavitree Formation. Older layers of the Heavitree Formation in the west are dominantly sourcing the Musgrave province whereas the successions on the east are dominantly sourcing the Aileron Province and Eastern Fold Belt from Mount Isa Province. The younger layers of the Heavitree formation have no spatial variance. All samples from the east and west show similar detrital zircon age spectra and ϵHf values in the range of Aileron Province and Eastern Fold Belt

data. Therefore, the Heavitree Formation dominantly sources the northern regions in the younger layers.

ACKNOWLEDGMENTS

I would like to acknowledge my primary supervisor Prof. Alan Collins his continuous support and understanding. I would like to thank my co-supervisor Dr. Morgan Blades for being extremely supportive throughout the year and always being there for help. I would like to acknowledge Northern Territory Geological Survey for funding this project. Huge thanks Dr. Justin Payne and Alec Walsh for their support in laboratory work. Many thanks to all my colleagues who came along to Alice Springs and helped in collecting my samples. Many thanks to Sarah from Adelaide Microscopy for her assistant and support with ICP-MS and microprobe work. Many thanks to Bo Yang for providing additional data to use in this research. The guidance and support throughout the year was amazing and greatly appreciated.

REFERENCES

- Ahmad, M. (2013). Chapter 25 Murraba Basin. *Geology and mineral resources of the Northern Territory compiled by M Ahmad and TJ Munson: Northern Territory Geological Survey, Darwin, Northern Territory, Special Publication, 5, 25-1.*
- Blades, M. (2013). *The age and origin of the western Ethiopian Shield* (Doctoral dissertation).
- Camacho, A., Armstrong, R., Davis, D. W., & Bekker, A. (2015). Early history of the Amadeus Basin: implications for the existence and geometry of the Centralian Superbasin. *Precambrian Research, 259, 232-242.*
- Close, D. F. (2013). Chapter 21: Musgrave Province. *Geology and mineral resources of the Northern Territory compiled by M Ahmad and TJ Munson: Northern Territory Geological Survey, Darwin, Northern Territory, Special Publication, 5, 21-1.*
- Corfu, F., Hancher, J. M., Hoskin, P. W., & Kinny, P. (2003). Atlas of zircon textures. *Reviews in mineralogy and geochemistry, 53(1), 469-500.*
- Da Silva, L. C., Hartmann, L. A., McNaughton, N. J., & Fletcher, I. (2000). Zircon U-Pb SHRIMP dating of a Neoproterozoic overprint in Paleoproterozoic granitic-gneissic terranes, southern Brazil. *American Mineralogist, 85(5-6), 649-667.*

- Edgoose, C. J. (2012). The Amadeus Basin, Central Australia. *Episodes*, 35(1), 256-263.
- Edgoose, C. J. (2013). Chapter 23: Amadeus Basin. *Geology and Mineral Resources of the Northern Territory, NTGS Special Publication*, 5, 23.
- Fedo, C. M., Sircombe, K. N., & Rainbird, R. H. (2003). Detrital zircon analysis of the sedimentary record. *Reviews in Mineralogy and Geochemistry*, 53(1), 277-303.
- Finch, R. J., & Hanchar, J. M. (2003). Structure and chemistry of zircon and zircon-group minerals. *Reviews in mineralogy and geochemistry*, 53(1), 1-25.
- Griffin, W. L., Belousova, E. A., Walters, S. G., & O'Reilly, S. Y. (2006). Archaean and Proterozoic crustal evolution in the Eastern Succession of the Mt Isa district, Australia: U–Pb and Hf-isotope studies of detrital zircons. *Australian Journal of Earth Sciences*, 53(1), 125-149.
- Hoskin, P. W., & Ireland, T. R. (2000). Rare earth element chemistry of zircon and its use as a provenance indicator. *Geology*, 28(7), 627-630.
- Hoskin, P. W., & Schaltegger, U. (2003). The composition of zircon and igneous and metamorphic petrogenesis. *Reviews in mineralogy and geochemistry*, 53(1), 27-62.
- HOWARD K. E., *et al.* 2009 Detrital zircon ages: Improving interpretation via Nd and Hf isotopic data, *Chemical Geology*, vol. 262, no. 3, pp. 277-292.
- Howard, K. E., Hand, M., Barovich, K. M., Reid, A., Wade, B. P., & Belousova, E. A. (2009). Detrital zircon ages: improving interpretation via Nd and Hf isotopic data. *Chemical Geology*, 262(3-4), 277-292.
- Job, A. L. (2011). *Evolution of the basal Adelaidean in the northern Flinders Ranges: deposition, provenance and deformation of the Callanna and lower Burra Groups* (Doctoral dissertation).
- Kruse, P. D., Dunster, J. N., & Munson, T. J. (2013). Chapter 28: Georgina Basin. *Ahmad, M. and Munson, TJ (compilers) Geology and Mineral Resources of the Northern Territory. Northern Territory Geological Survey, Special Publication*, 5.
- Latkoczy, C., & Ghislain, T. (2006). Simultaneous LIBS and LA-ICP-MS analysis of industrial samples. *Journal of analytical atomic spectrometry*, 21(11), 1152-1160.
- Munson, T., Kruse, P., & Ahmad, M. (2013). Chapter 22: Centralian Superbasin. *Geology and mineral resources of the Northern Territory compiled by M Ahmad and TJ Munson: Northern Territory Geological Survey, Darwin, Northern Territory, Special Publication*, 5, 22-1.

- Nemchin, A. A., & Cawood, P. A. (2005). Discordance of the U–Pb system in detrital zircons: implication for provenance studies of sedimentary rocks. *Sedimentary Geology*, 182(1-4), 143-162.
- Ozimic, S., Passmore, V. L., Pain, L., & Levering, I. H. (1986). Australian Petroleum Accumulations Report 1, Amadeus Basin, Central Australia, Australia. *Bureau of Mineral Resources, Canberra*, 64.
- PAYNE J. L., PEARSON N. J. & GRANT K. H., G.P 2013 Reassessment of relative oxide formation rates and molecular interferences on in-situ Lutetium-Hafnium analysis with Laser Ablation MC-ICP-MS. , *Journal of Analytical Atomic Spectrometry* vol. 28, no. 7, pp. 1068-1079.
- Scrimgeour, I. R. (2013). Chapter 12: Aileron Province: in Ahmad M and Munson TJ (compilers) 'Geology and Mineral Resources of the Northern Territory'. *Northern Territory Geological Survey, Special Publication*, 5.
- Scrimgeour, I. R. (2013). Chapter 13: Warumpi Province. *Geology and mineral resources of the Northern Territory compiled by M Ahmad and TJ Munson: Northern Territory Geological Survey, Darwin, Northern Territory, Special Publication*, 5, 13-1.
- Vermeesch, P., 2018, IsoplotR: a free and open toolbox for geochronology. *Geoscience Frontiers*, doi: 10.1016/j.gsf.2018.04.001.
- Wade, B. P., Kelsey, D. E., Hand, M., & Barovich, K. M. (2008). The Musgrave Province: stitching north, west and south Australia. *Precambrian Research*, 166(1-4), 370-386.
- Yang, B., Smith, T. M., Collins, A. S., Munson, T. J., Schoemaker, B., Nicholls, D., ... & Glorie, S. (2018). Spatial and temporal variation in detrital zircon age provenance of the hydrocarbon-bearing upper Roper Group, Beetaloo Sub-basin, Northern Territory, Australia. *Precambrian Research*, 304, 140-155.

APPENDIX A: GEOCHRONOLOGY

Mineral Separation

Crushing

1. Cut the rocks using the rock saw.
2. Make sure that the rocks are dry, clean and fresh. Ensuring that there is no lichen or texta left on the rocks.
3. Clean the jaw crusher before and after use
 - a. This is done using compressed air and ethanol.
4. Line the tray with butcher paper to ensure that the samples are not contaminated.
5. The disc mill is used to achieve the zircon fraction. Clean the machine using compressed air and ethanol.
6. Move the discs until the desired gap is reached. Start at 1mm.
7. Run this through the sieve using $<79 \mu\text{m}$ and $>479 \mu\text{m}$ mesh. Place the sieve into the Endcotts EPL2000 Super Shaker and allow for the fractions to separate.
8. Take the course fraction $>479 \mu\text{m}$ and run it through the disc mill again, changing the spacing between the discs to 0.7mm.
9. Repeat this process again with the spacing at 0.4mm.
10. Put each fraction into the sample bags. Labelling ' $>479 \mu\text{m}$ ', 'Zircon fraction' and ' $<79 \mu\text{m}$ '
11. If samples are undergoing geochemistry, after they have been through the jaw crusher they are placed into the ring mill using the tungsten carbide. The ring mill is cleaned with compressed air and ethanol.
12. Quartz blank is first used to ensure contamination is kept at a minimum. The quartz is run for 1.5 minutes.
13. The samples are then placed into the tungsten carbide mill and run for 3 minutes.
14. This fraction is then placed in a sample bag for later requirements.

Separating the zircons from the 'zircon fraction'

The separation was done in the Mawson Building lab B29 at Adelaide University.

Before each use the room is cleaned before each use. The benches are cleaned and the room is vacuumed.

The sample is panned removing the lights from the fraction. The lights are placed into a funnel with filter paper and later dried in the oven.

The heavies extracted by this method are the placed on the hotplate to dry at $50 \text{ }^\circ\text{C}$. To separate the magnetic material the sample is put through the FRANZ.

For the first time the sample is run through at 1.0 amps. This will separate the highly magnetic minerals.

This is repeated. The magnet is turned up to 1.6 amps. Each magnetic fraction is placed in a sample bag and clearly labelled.